Hindawi Publishing Corporation
Advances in Astronomy
Volume 2012, Article ID 782528, 11 pages
doi:10.1155/2012/782528

Research Article

The Low-Mass End of the $M_{\mathrm{BH}}/M_{\mathrm{host}}$ Relation in Quasars

Roberto Decarli,[1] Renato Falomo,[2] Jari K. Kotilainen,[3] Tomi Hyvönen,[3] Michela Uslenghi,[4] and Aldo Treves[4,5,6]

[1] *Galaxy and Cosmology Department, Max-Planck-Institut für Astronomie, Königstuhl 17, 69117 Heidelberg, Germany*
[2] *Osservatorio Astronomico di Padova, INAF, Vicolo dell' Osservatorio 5, 35122 Padova, Italy*
[3] *Finnish Centre for Astronomy with ESO (FINCA), University of Turku, Väisäläntie 20, 21500 Piikkiö, Finland*
[4] *INAF-IASF Milano, Via E. Bassini 15, 20133 Milano, Italy*
[5] *Dipartimento di Fisica e Matematica, Università degli Studi dell'Insubria, Via Valleggio 11, 22100 Como, Italy*
[6] *INFN Milano-Bicocca, Dipartimento di Fisica University, Milano Bicocca, Piazza della Scienza 3, I-20126 Milano, Italy*

Correspondence should be addressed to Roberto Decarli, decarli@mpia.de

Received 28 July 2011; Accepted 4 October 2011

Academic Editor: Angela Bongiorno

The M_{BH}-M_{host} relation in quasars has been probed only in a limited parameter space, namely, at $M_{\mathrm{BH}} \sim 10^9$ $\mathrm{M}_\odot$ and $M_{\mathrm{host}} \sim 10^{12}$ $\mathrm{M}_\odot$. Here we present a study of 26 quasars laying in the low-mass end of the relation, down to $M_{\mathrm{BH}} \sim 10^7$ $\mathrm{M}_\odot$. We selected quasars from the SDSS and HST-FOS archives, requiring modest M_{BH} (as derived through the virial paradigm). We imaged our sources in H band from the Nordic Optical Telescope. The quasar host galaxies have been resolved in 25 out of 26 observed targets. Host galaxy luminosities and stellar masses are computed, under reasonable assumptions on their star formation histories. Combining these results with those from our previous studies, we manage to extend the sampled parameter space of the M_{BH}-M_{host} relation in quasars. The relation holds over 2 dex in both the parameters. For the first time, we are able to measure the slope of the M_{BH}-M_{host} relation in quasars. We find that it is consistent with the linear case (similarly to what observed in quiescent galaxies). We do not find any evidence of a population of massive black holes lying below the relation.

1. Introduction

Massive black holes (BHs) are ubiquitously found in the centre of massive galaxies [1–3]. Their masses (M_{BH}) show strong correlations with large-scale properties of the host galaxies, namely, the stellar velocity dispersion (σ_*, [4–7]), the luminosity, and mass of the spheroidal component (L_{host}, M_{host}; see [8–10]). These relations have been interpreted as the outcome of a joint evolution between BHs and their host galaxies [11–18]. In this scenario, the growth of BHs through accretion regulates the gas cooling in the outskirt of host galaxies through energy or momentum injection (feedback), thus quenching the formation of stars. Galaxy mergers may also play a role in this scenario, as gravitationally induced dynamical instabilities may trigger both star formation bursts and gas inflows fuelling the BH activity ([12, 19–21], see also [22]).

The M_{BH}-host galaxy relations have been pinned down on an albeit small set of local, mostly quiescent galaxies. The sampled parameter space ranges over 3 dex in masses, from a few million to a few billion solar masses in terms of M_{BH}. Extending these studies beyond the local Universe is challenging. On one side, the influence radius of BHs, R_{inf}, that is, the radius where the gravitational potential is dominated by the singularity, is resolved only in very nearby objects (distances < few tens Mpc) with high M_{BH} values. For any other sources, indirect tracers of M_{BH} are required. The most commonly adopted indirect estimator of M_{BH} is based on the width of broad emission lines and the size of the broad line region (BLR). This can be done only in type-1 AGN, where broad lines are observed [23–26]. This approach allows to estimate M_{BH} from single-epoch spectra in ~100 000 quasars up to $z \sim 5$ from SDSS spectra [27], and in most of the $z \sim 6$ quasars known to day [28–31]. (Caveats to this technique arise as BLR clouds may be supported by radiation pressure [32] or move nonvirially; projection effects depending on the geometry and orientation of the BLR may hinder our ability to actually measure the orbital velocity of clouds [33, 34]; different emission lines may be produced in regions where the gas dynamics are different [35–39].)

On the other side, the properties of host galaxies are hard to measure in distant sources. Bright active nuclei (necessary to measure $M_{\rm BH}$) can easily outshine the light of their host galaxies. Observations in excellent seeing conditions (e.g., [40, 41])or based on adaptive optics (e.g., [42, 43]) are required. Diffraction-limited observations with HST have also significantly contributed in this field [44–54], although some concerns about the reproducibility of the PSF have been arisen [51]. Up to now, ~ 300 quasar host galaxies have been resolved up to $z \approx 3$, and most of them at $z < 0.5$ (see [40], and references therein).

In order to understand the processes and timescales which led to the onset of the BH-host galaxy relations, two key observational tests are required. The first one consists in *tracing the evolution of the* BH*-to-host galaxy mass ratio (*$\Gamma \equiv M_{\rm BH}/M_{\rm host}$*) as a function of Cosmic Time*. If, for example, $\Gamma(z > 0) < \Gamma(z \approx 0)$, then we can argue that the BHs in these systems still have to accrete in already formed bulges. Vice versa, $\Gamma(z > 0) > \Gamma(z \approx 0)$ could suggest a rapid growth of the BHs, followed by a slower build-up of the spheroids. Most of the studies on the evolution of the BH-host galaxy relations suggest that at high redshift, for a given mass of the host spheroid, the harbored BH is more massive than at low-z [50, 53, 55–58], with $\Gamma(z) \propto (1 + z)^{3/2}$. It is interesting to note that the host galaxy of J1148 + 5251, the highest-z SDSS quasar, at $z = 6.42$, shows an $M_{\rm BH}$-host galaxy dynamical mass ratio of ≈ 0.13 [59, 60], in an order-of-magnitude agreement with the extrapolation from the $z < 3$ studies.

A second observational test to probe the onset of the BH-host galaxy relations is to *trace the low-mass end of the BH-host galaxy relations*. Different initial host galaxy mass, BH seed mass, and build-up processes produce different slopes of the relations, especially at low mass. Light seeds ($10 - 100\,{\rm M}_\odot$) are expected as the remnants of metal-pure stars in the early Universe, while heavier seeds (up to $\sim 10^5\,{\rm M}_\odot$) can result from the direct collapse of primordial gas clouds. The former ones would produce a larger scatter in the $M_{\rm BH}$-host relations, a higher occupation fration in relatively small galaxies, and a lower cutoff in the minimum $M_{\rm BH}$ with respect to the latter (see, e.g., [61], and references therein). Some authors even claim that the $M_{\rm BH} - \sigma_*$ relation itself is just the upper limit of a broader distribution, with a number of (hard-to-detect) modest-mass BHs embedded in relatively massive galaxies (e.g., [62]).

The low-mass end of the $M_{\rm BH}$-host galaxy relations has been probed down to few 10^5 $M_{\rm BH}$ in quiescent galaxies or in low-luminosity AGN at low-z [54, 63–67], suggesting that the $M_{\rm BH}$-host relations hold in quiescent or mildly active galaxies. However, no effort has been attempted so far to extend this test to higher luminosity AGN. Quasars are ideal probes of the BH-host galaxy relations at $z > 0$. However, while Γ in quasars has been measured up to very high redshift, the ranges of $M_{\rm BH}$ and $M_{\rm host}$ investigated up to date are limited, and comparable with the observed scatter of the BH-host galaxy relations. Filling the low-mass end of the $M_{\rm BH}$-$M_{\rm host}$ relation therefore represents a main challenge and a fundamental step in our comprehension of the BH-host galaxy evolution. In this paper, we present ground-based NIR observations of quasars at $z < 0.5$ selected so that virial $M_{\rm BH} < 10^9$ $M_{\rm BH}$. Our imaging campaign successfully resolved 25 quasar host galaxies. This enables us to directly probe the slope of the $M_{\rm BH}$-$M_{\rm host}$ relation in quasars.

The structure of this work is the following: in Section 2 we describe the sample. In Section 3 we present the analysis of the spectra and we derive $M_{\rm BH}$ in all our sources. The new observations, the data reduction and analysis, and the results from the imaging campaign are presented in Section 4. In Section 5 we discuss our results. Conclusions are summarized in Section 6. Throughout the paper we will assume a standard cosmology with $H_0 = 70\,{\rm km s^{-1}\,Mpc^{-1}}$, $\Omega_{\rm m} = 0.3$, and $\Omega_\Lambda = 0.7$.

2. The Sample

We selected quasars at $z < 0.5$ with available Hβ observations in the Sloan Digital Sky Survey (SDSS [68]) spectroscopic database or $C_{\rm IV}$ or $Mg_{\rm II}$ observations in the HST-Faint Object Spectrograph (FOS) archive. We require that black hole virial masses, computed as described in Section 3, range between 10^7 and $10^9\,{\rm M}_\odot$. Note that, out of the 62 $z < 0.5$ quasars examined in our previous study [26], only 8 (13%) had $M_{\rm BH} < 10^9\,{\rm M}_\odot$. We then selected quasars having at least 3 relatively bright ($m_H = 10$–15 mag) stars within 2′ (corresponding to the half size of the NOTCam field of view), and a number of fainter stars in order to have an accurate description of the Point Spread Function (PSF). Observability constraints and modest weather losses further limited our analysis to 26 targets (see Table 1), mostly detected in radio wavelengths according to the [69] catalogue. This new sample is then matched with the 62 $z < 0.5$ targets presented in our previous study of the $M_{\rm BH}$-$M_{\rm host}$ relation [26, 58]. Figure 1 compares the distribution of $M_{\rm BH}$ in the general SDSS sample at $z < 0.5$, computed from the continuum luminosities and Hβ width estimates reported by [27], with the ones presented in [26] and in the present study.

3. The Spectroscopic Dataset

The spectroscopic dataset consists of pipeline-processed, publicly available spectra from the SDSS or FOS archive. SDSS spectra have $\lambda/\Delta\lambda \sim 2000$ and a spectral range between 3800 and 9000 Å. Uncertainties on wavelength calibration amount to 0.05 Å, while flux calibration formal errors account to 5%. FOS spectra are taken from the compilation of recalibrated quasar and AGN FOS spectra by [70]. Observations were performed with a number of different gratings at both high spectral resolution (1–6 Å diode^{-1}, $\lambda/\Delta\lambda \approx 1300$) and low spectral resolution (6–25 Å diode^{-1}, $\lambda/\Delta\lambda \approx 250$) covering various spectral windows from 1140 Å to 3275 Å. Photometric uncertainties are usually 5–10%, while typical wavelength calibration uncertainties are around 0.5 channels rms (see [70]).

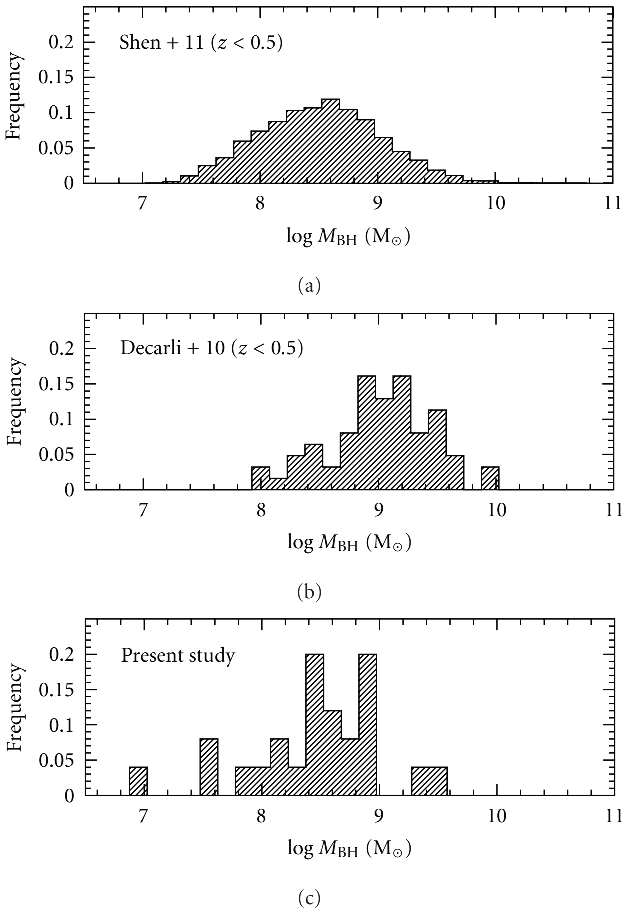

Figure 1: Comparison among the M_{BH} distributions in the SDSS quasars at $z < 0.5$ [27] (a), in our 2010 study (b) and in the present work (c). The latter is clearly more representative of the general quasar population at low redshift.

Table 1: The sample. (1) Target name. (2-3) Right ascension and declination (J2000). (4) Is the target detected in radio wavelengths, according to the [69] catalogue? (5) Catalogue redshift. (6) Apparent visual magnitude of the quasar.

Name	RA	DEC	Radio?	z	V [mag]
(1)	(2)	(3)	(4)	(5)	(6)
PB5723	00 05 47.5	+02 03 02	N	0.234	16.60
PG0026 + 12	00 29 13.7	+13 16 04	Y	0.145	15.41
PG0052 + 251	00 54 52.1	+25 25 39	Y	0.155	15.43
B20110 + 29	01 13 24.2	+29 58 16	Y	0.363	17.00
PKS0214 + 10	02 17 07.6	+11 04 10	Y	0.408	16.46
J02321 + 0008	02 32 11.8	+00 08 03	Y	0.432	19.10
J02331 − 0909	02 33 10.6	−09 09 40	Y	0.388	18.45
J03010 + 0004	03 01 00.2	+00 04 29	Y	0.486	19.33
J03323 + 0106	03 32 18.0	+01 06 48	N	0.482	18.91
J03579 − 0550	03 57 59.0	−05 50 15	Y	0.439	18.93
B20752 + 25*A*	07 55 37.0	+25 42 39	Y	0.446	18.00
J08044 + 1904	08 04 42.1	+19 04 26	Y	0.346	19.40
J08285 + 2748	08 28 53.5	+27 48 33	N	0.330	20.00
J08305 + 0802	08 30 57.4	+08 02 34	Y	0.319	19.20
PG0844 + 349	08 47 42.4	+34 45 03	Y	0.064	14.50
J09010 + 3538	09 01 00.9	+35 38 09	N	0.302	19.20
PG0947 + 396	09 50 48.3	+39 26 51	Y	0.206	16.39
PG0953 + 415	09 56 52.4	+41 15 23	Y	0.234	15.32
TON1187	10 13 03.1	+35 51 23	N	0.079	14.75
TEX1156 + 213	11 59 26.2	+21 06 56	Y	0.349	16.90
Q1214 + 1804	12 16 49.0	+17 48 04	N	0.374	17.30
PG1404 + 226	14 06 21.9	+22 23 47	Y	0.098	15.82
PG1415 + 451	14 17 00.8	+44 56 06	Y	0.114	15.24
PG1626 + 554	16 27 56.1	+55 22 31	Y	0.132	15.68
4C73.18	19 27 48.5	+73 58 02	Y	0.302	16.50
PKS2251 + 11	22 54 10.4	+11 36 39	Y	0.325	15.82

Spectral analysis follows the same approach described in [26] and [31]. Briefly, continua are modeled as a superposition of a power-law component, the host galaxy emission (only in the optical spectra; the Elliptical model by [71] was adopted as a template), and the Fe_{II} multiplets (modeled on the template by [72]). Relevant broad emission lines (Hβ, Mg_{II}, and C_{IV}) are modeled with the superposition of two Gaussian curves with the same peak wavelength. The spectral resolution of the SDSS data is adequate to allow an easy identification of the narrow Hβ emission with respect to the broad line. Examples of the line fitting are shown in Figure 2.

We measure the continuum luminosity at 1350, 3000, and 5100 Å from the fitted power-law. The broad line luminosity and FWHM are measured from the line model (see [36], for a discussion on the fitting technique and the parametrization of the relevant quantities). Virial black hole masses are computed with the same recipes used in [26], adopting geometrical factors of 1.6 for Hβ and Mg_{II} and 2.4 for C_{IV}. Table 2 lists the main measurements and inferred quantities from the spectroscopic analysis. (We note that, after a careful reanalysis of the spectra, two objects (B20110+29 and B20752 + 25*A*) show values of M_{BH} slightly exceeding the initial selection criteria. Nevertheless, we include these sources in the present analysis.)

4. The Imaging Dataset

All the objects in our study have been observed in *H* band in a campaign at the 2.5 m Nordic Optical Telescope (Roque de Los Muchachos, Spain) using NOTCam. Observations were carried out during three observing runs in May 2007 and April and November 2008. The average seeing in *H* band was $0.7''$. The 1024 × 1024 pixel NOTCam detector has a pixel scale of $0.235''$ pxl^{-1}, yielding a field of view size of ~4 × 4 $arcmin^2$. Usual observing techniques for broad-band NIR imaging of point-like sources were adopted. Observations were split in 1 min long individual frames. Random jittering patterns within a $20''$ box were adopted in order to perform optimal sky subtraction. The total time on each source was 45 min.

Data reduction was performed using IRAF. (IRAF is distributed by the National Optical Astronomy Observatories, which are operated by the Association of Universities for Research in Astronomy, Inc., under cooperative agreement

Table 2: Results from the spectroscopic analysis. (1) Quasar name. (2) Redshift. (3) Line used in the M_{BH} estimate. (4) Continuum monochromatic luminosity at 1350 (for C_{IV}), 3000 (for Mg_{II}) or 5100 Å (for Hβ), in ergs^{-1}. (5) Line FWHM in km s^{-1}. (6) Virial estimate of the black hole mass, in solar units.

Name (1)	z (2)	Line (3)	$\log \lambda L_\lambda$ [erg s^{-1}] (4)	FWHM [km s^{-1}] (5)	$\log M_{BH}$ [$M_\odot$] (6)
PB5723	0.234	C_{IV}	44.71	3715	8.15
PG0026 + 12	0.145	C_{IV}	45.22	2062	7.92
PG0052 + 251	0.155	C_{IV}	45.33	5914	8.90
B20110 + 29	0.363	Hβ	44.81	6149	9.33
PKS0214 + 10	0.408	C_{IV}	45.71	4122	8.79
J02321 + 0008	0.432	Hβ	44.41	1727	7.56
J02331 − 0909	0.388	Hβ	44.63	1863	7.77
J03010 + 0004	0.486	Hβ	44.45	6634	8.76
J03323 + 0106	0.482	Hβ	44.77	4282	8.59
J03579 − 0550	0.439	Hβ	44.62	4005	8.43
B20752 + 25*A*	0.446	Hβ	45.06	9738	9.50
J08044 + 1904	0.346	Hβ	44.09	7322	8.60
J08285 + 2748	0.330	Hβ	44.14	5385	8.37
J08305 + 0802	0.319	Hβ	44.14	6149	8.48
PG0844 + 349	0.064	Mg_{II}	44.57	3209	8.20
J09010 + 3538	0.302	Hβ	44.29	8495	8.86
PG0947 + 396	0.206	C_{IV}	45.17	4090	8.49
PG0953 + 415	0.234	C_{IV}	45.45	3490	8.50
TON1187	0.079	Hβ	44.20	2141	7.60
TEX1156 + 213	0.349	Hβ	44.93	5663	8.94
Q1214 + 1804	0.374	Hβ	45.04	3728	8.65
PG1404 + 226	0.098	Hβ	44.14	1036	6.93
PG1415 + 451	0.114	Hβ	44.19	3244	7.96
PG1626 + 554	0.132	C_{IV}	45.18	4057	8.49
4C73.18	0.302	C_{IV}	45.92	4155	8.91
PKS2251 + 11	0.325	C_{IV}	45.54	5028	8.87

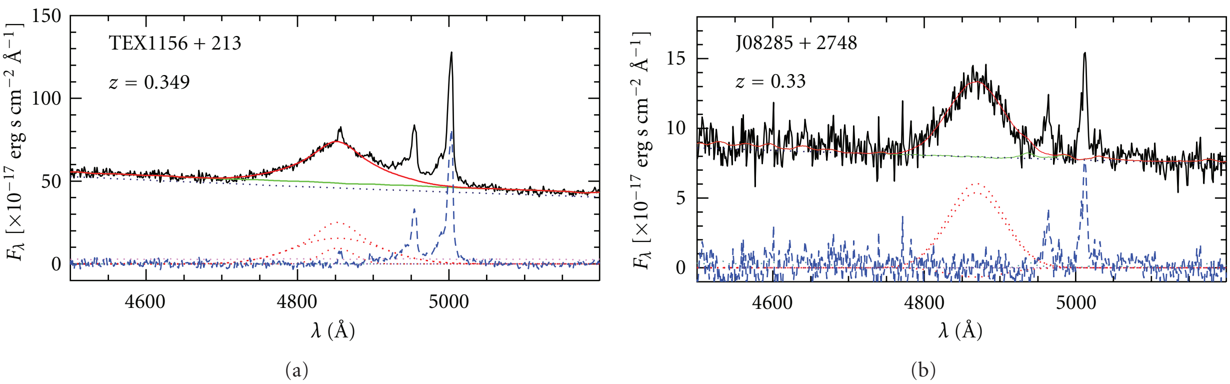

Figure 2: Examples of Hβ line fitting. The observed spectra, shifted to the rest frame, are plotted in solid, black lines. The various components of the models are shown: the power-law (black, dotted line), the host galaxy and Fe_{II} templates (green, solid line), the line model (red, solid line), and its components (red, dotted lines). Fit residuals are shown in blue, dashed lines.

with the National Science Foundation.) Bad pixels were corrected for in each image using a mask made from the ratio of two sky flats with different illumination levels. Sky subtraction was performed for each science image using a median averaged frame of all the other temporally close frames in a grid of eight exposures. Flat fielding was made using normalized median averaged twilight sky frames with different illumination levels. Finally, images were aligned to subpixel accuracy using field stars as reference points and combined after removing spurious pixel values to obtain the final reduced coadded image. Zero point calibration is achieved by cross-matching the photometry of field stars with the 2MASS database. This approach yields typical photometric uncertainties <0.1 mag.

We analyzed our data using the Astronomical Image Decomposition and Analysis package (AIDA; [73]), an IDL-based software designed to perform two-dimensional model fitting of quasar images. Details on the procedure are presented in [40, 74] and briefly summarized here.

A careful modeling of the Point Spread Function (PSF) is crucial to disentangle the extended host galaxy light from the nuclear source. To model the PSF shape, we used suitable field stars. Each star was modeled with four two-dimensional Gaussians, representing the core of the PSF, and an exponential feature, representing the extended wing of the PSF. Regions contaminated by nearby sources, saturated pixels, and other defects affecting the images were masked out.

In order to discriminate between resolved and unresolved targets, we first fit the images of our sources with the pure PSF model. In most of the cases, an extended halo was clearly observed in the residuals. We then reperformed the fits using a Sersic law, (describing the host galaxy) plus a point-source (the nucleus), convolved to the PSF model. In all but one case (J02331 − 0909), this second fit is significantly better than the fit with the pure PSF, as confirmed by the χ^2 ratio between the two fits (see Table 3).

An example of the outputs of our analysis is shown in Figure 3.

Host galaxy apparent H-band magnitudes are then converted into rest-frame R-band. We use the Elliptical galaxy template by [71] to estimate k-corrections. The host galaxy R-band absolute magnitude is then converted into a stellar mass by adopting the mass-to-light ratio (M/L) of a single stellar population originated at $z_{\text{burst}} = 5$ and passively evolving down to $z = 0$ (see [58], for details). Table 3 summarizes the relevant results from the modeling of the quasar host galaxies described here.

5. Discussion

In Figure 4 we show the M_{BH}-M_{host} relation for quasar host galaxies at $z < 0.5$. The dataset (62 objects from [26, 58], plus 25 objects with resolved host galaxies from the present study) span over 2 dex in both M_{BH} and M_{host}. The same M_{BH}-M_{host} relation observed for inactive galaxies appears to hold through all the sampled range, from $\sim 3\times10^{10}$ to $\sim 3\times10^{12}\,\text{M}_\odot$ in terms of M_{host}. We find that $\langle \log \Gamma \rangle = -2.843$ (in excellent agreement with the $M_{\text{BH}} = 0.0015\,M_{\text{host}}$ value reported by [9], for inactive galaxies) with a 0.44 dex scatter. Only 3 sources (J02321+0008, PG1404+226 from this study; 1001 + 291 from the old sample) lie more than 2-σ *below* the relation. Since the sampled parameter space is about 5 times larger than the dispersion of the relation, we can exclude that the observed M_{BH}-M_{host} relation is the upper envelope of a population of quasars with relatively small black holes hosted by very massive galaxies. The best bilinear regression fit of the relation is

$$\log \frac{M_{\text{BH}}}{10^9\,\text{M}_\odot} = (1.26 \pm 0.29) \times \log \frac{M_{\text{host}}}{7\cdot 10^{11}\,\text{M}_\odot} + (0.04 \pm 0.03), \qquad (1)$$

consistent with the relations with a constant $M_{\text{BH}}/M_{\text{host}}$ ratio, as observed in quiescent galaxies in the local Universe [9, 10].

When considering subsets of our data, the high-mass end shows a slightly smaller scatter (see Table 4).

For twelve objects the host galaxies are found to be best described by a Sersic law with small index ($n_{\text{s}} < 1.5$), suggesting the presence of significant disc components. In particular, PG1404 + 226 (incidentally, the object showing the smallest M_{BH} and the largest deviation with respect to the M_{BH}-M_{host} relation in our sample) shows clear spiral arms in the residuals of the host galaxy model. From local galaxy studies, M_{BH} is found to be more sensitive to the properties of the spheroidal stellar component rather than of the whole galaxy. On the other hand, a bulge + disc decomposition is practically impossible with ground-based images of quasar host galaxies at relatively high redshift. Here we attempt a rule-of-thumb correction starting from the Sersic index value. We assume that the bulge-to-total luminosity ratio in the rest-frame R band, B/T, scales with the Sersic index as follows:

$$B/T = \begin{cases} (n_{\text{s}} - 0.5)/3.5 & \text{if } n_{\text{s}} < 4, \\ 1 & \text{if } n_{\text{s}} \geq 4. \end{cases} \qquad (2)$$

This simple analytical form roughly traces the bulk of the B/T values for $n_{\text{s}} < 4$, as found by [75], who performed accurate image deconvolution for $\sim$1 million galaxies from the SDSS. Furthermore, it is consistent with the operative hypothesis that all the galaxies well described by a de Vaucouleurs profile ($n_{\text{s}} = 4$) are bulge dominated ($B/T \approx 1$), as assumed in our previous study. The effect of this correction is to move disc-dominated host galaxies towards the left side of Figure 4. In particular, all but one source at $M_{\text{bulge}} < 10^{10}\,\text{M}_\odot$ would lie *above* the local relation. The best fit relation is indeed flatter (0.88 ± 0.18 instead of 1.26 ± 0.29), but still consistent with the linear case. The scatter is also increased (0.53 dex, computed over the whole sample; 0.61 and 0.55 dex in the small M_{BH} and small M_{bulge} subsets, resp.). We stress that the correction reported in (2) is uncertain, because of the wide range of B/T values reported for any given n_{s}. However, we remark that any correction for the B/T would make the case against a population of under-massive black holes in very massive galaxies even stronger.

A similar argument can be used to evaluate how our results are affected by different assumptions on the star formation history. In our study, we adopted the mass-to-light ratio (M/L) of a single stellar population originated at $z_{\text{burst}} = 5$ and passively evolving down to $z = 0$. However, objects with significant disc contaminations are expected to have a younger stellar population than old, passive spheroids. This would imply smaller M/L, that is, less massive host galaxies for a given observed host luminosity. This would make the case against a quasar population lying *below* the observed M_{BH}-M_{host} relation even more robust.

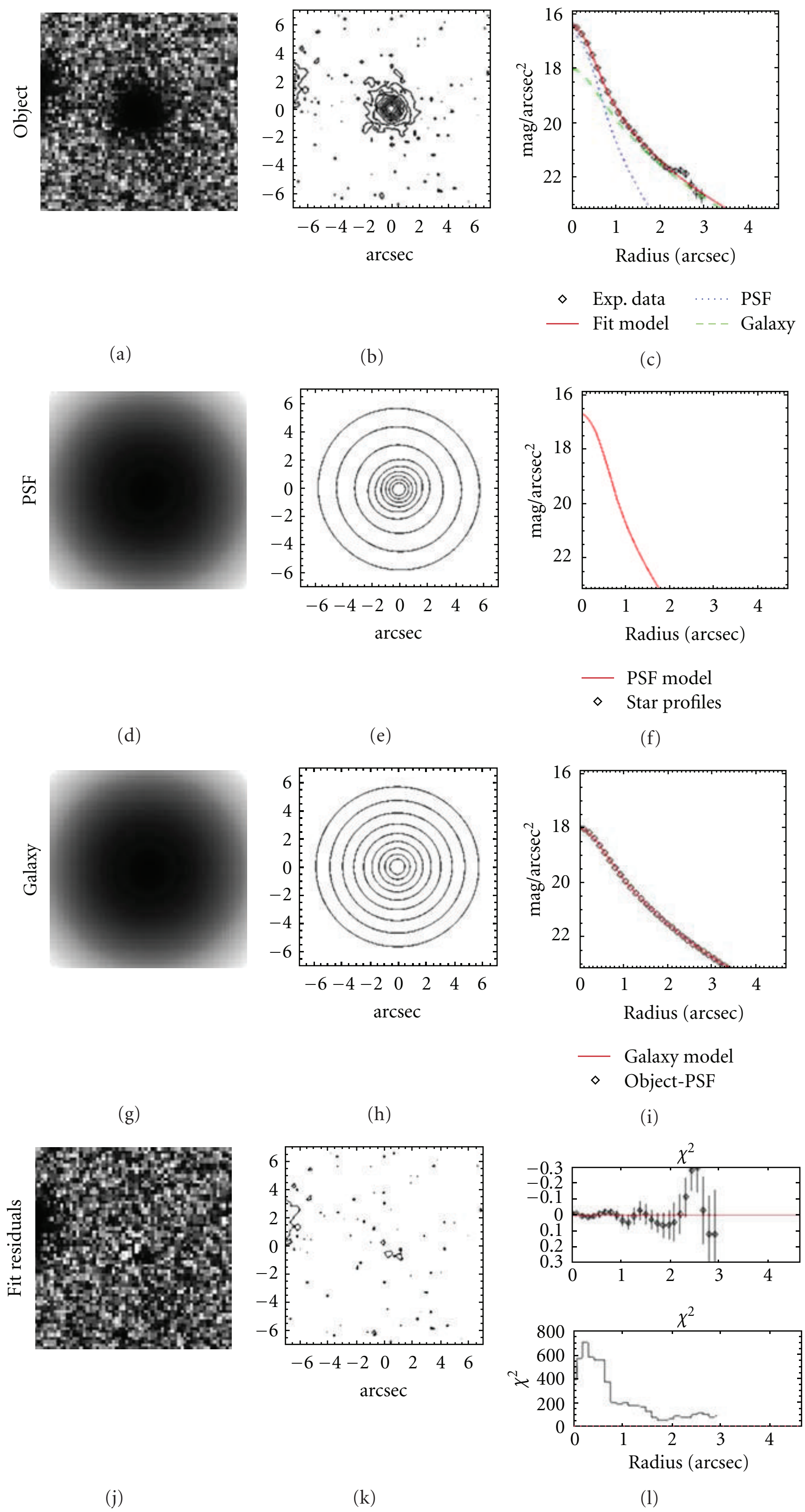

FIGURE 3: An example of the analysis of the quasar host galaxies, shown in the case of the quasar J08285 + 2748. *Top panels:* observed quasar image (left), contour plot (center), and light profile (right; the PSF and galaxy models are plotted in dotted and dashed lines, resp.). *Central panels:* similarly, the images (left), contour plots (center), and light profile (right) of the PSF and the galaxy model. *Bottom panels:* image (left), contour plot (center), and light profile (top right) of residuals after model subtraction. The radial distribution of χ^2 values is also plotted (bottom right).

TABLE 3: Results from the imaging analysis. (1) Quasar name. (2) Redshift. (3) Apparent observed H-band magnitude of the nucleus. (4) Apparent observed H-band magnitude of the host galaxy. (5) Apparent central surface brightness, as extrapolated from the host galaxy model. (6) Chi-square ratio between the best fit using a pure PSF and the best fit using a galaxy+quasar model. (7) Effective radius of the host galaxy. (8) Ellipticity of the host galaxy model. (9) Sersic index of the host galaxy model. (10) Rest-frame R-observed H color correction. (11) Resulting absolute rest-frame R-band magnitude of the host galaxy. (12) Adopted mass-to-light ratio. (13) Stellar mass of the host galaxy. (14) BH-to-host galaxy mass ratio.

Name (1)	z (2)	$m_{\rm nuc}$ [mag] (3)	$m_{\rm host}$ [mag] (4)	μ_0 [mag $''^{-2}$] (5)	$\chi_{\rm psf}/\chi_{\rm gq}$ (6)	R_e (7)	Ell[$''$] (8)	n_s (9)	R-H [mag] (10)	$M_{\rm R}$ [mag] (11	log M/L [$M_\odot/L_\odot$] (12)	log $M_{\rm host}$[$M_\odot$] (13)	log Γ (14)
PB5723	0.234	15.99	15.81	5.41	1.41	0.32	0.57	5.00	2.59	−21.93	0.71	11.38	−3.61
PG0026 + 12	0.145	12.90	14.94	16.10	1.77	1.44	0.15	1.20	2.58	−21.64	0.75	11.30	−3.76
PG0052 + 251	0.155	13.46	14.37	16.34	6.55	2.19	0.19	1.22	2.58	−22.38	0.74	11.59	−3.07
B20110 + 29	0.363	16.04	16.21	12.07	2.51	3.89	0.09	5.00	2.60	−22.61	0.67	11.61	−2.48
PKS0214 + 10	0.408	14.60	16.10	13.98	1.88	1.16	0.00	2.77	2.59	−23.03	0.65	11.77	−3.36
J02321 + 0008	0.432	99.90	16.80	9.93	1.43	0.37	0.00	3.89	2.58	−22.50	0.64	11.54	−4.18
J02331 − 0909	0.388	15.98	—	—	1.01	—	—	—	—	—	—	—	—
J03010 + 0004	0.486	99.90	17.35	13.42	1.17	0.26	0.24	1.89	2.57	−22.25	0.63	11.43	−2.87
J03323 + 0106	0.482	18.66	17.15	11.55	1.91	0.54	0.61	3.17	2.57	−22.43	0.63	11.50	−3.11
J03579 − 0550	0.439	18.78	17.22	8.06	1.14	0.45	0.35	5.00	2.58	−22.12	0.64	11.39	−3.16
B20752 + 25A	0.446	14.80	16.14	12.51	1.39	0.71	0.07	2.95	2.58	−23.24	0.64	11.83	−2.53
J08044 + 1904	0.346	17.07	17.40	17.73	1.55	0.98	0.37	1.00	2.60	−21.30	0.67	11.09	−2.69
J08285 + 2748	0.330	16.98	17.20	16.63	1.58	0.81	0.06	1.53	2.60	−21.38	0.68	11.13	−2.96
J08305 + 0802	0.319	17.50	18.25	17.66	1.19	0.57	0.33	0.90	2.60	−20.25	0.68	10.68	−2.40
PG0844 + 349	0.064	13.34	14.59	17.55	1.92	2.82	0.27	0.90	2.56	−20.13	0.78	10.73	−2.73
J09010 + 3538	0.302	17.08	16.35	14.10	2.79	0.91	0.20	2.43	2.60	−22.01	0.69	11.39	−2.73
PG0947 + 396	0.206	14.42	15.18	16.17	4.45	1.92	0.20	1.59	2.59	−22.24	0.72	11.52	−3.41
PG0953 + 415	0.234	12.93	15.80	19.36	1.33	3.39	0.12	0.90	2.59	−21.93	0.71	11.38	−3.26
TON1187	0.079	13.97	14.95	16.83	3.70	1.91	0.20	1.10	2.56	−20.25	0.77	10.77	−3.37
TEX1156 + 213	0.349	15.38	15.78	14.86	2.50	1.07	0.12	1.98	2.60	−22.95	0.67	11.75	−3.01
Q1214 + 1804	0.374	16.36	16.48	12.05	1.11	0.25	0.40	1.97	2.59	−22.44	0.66	11.54	−3.09
PG1404 + 226	0.098	14.35	14.70	17.08	7.62	2.99	0.52	1.04	2.57	−20.97	0.77	11.05	−4.32
PG1415 + 451	0.114	13.65	14.02	15.22	10.56	1.50	0.04	1.30	2.57	−22.01	0.76	11.46	−3.70
PG1626 + 554	0.132	13.80	14.78	16.23	8.55	2.04	0.04	1.53	2.57	−21.60	0.75	11.29	−3.18
4C73.18	0.302	13.55	16.42	17.58	1.44	1.16	0.18	0.90	2.60	−21.94	0.69	11.36	−2.83
PKS2251 + 11	0.325	13.53	15.70	18.62	2.94	2.43	0.05	0.90	2.60	−22.86	0.68	11.72	−3.23

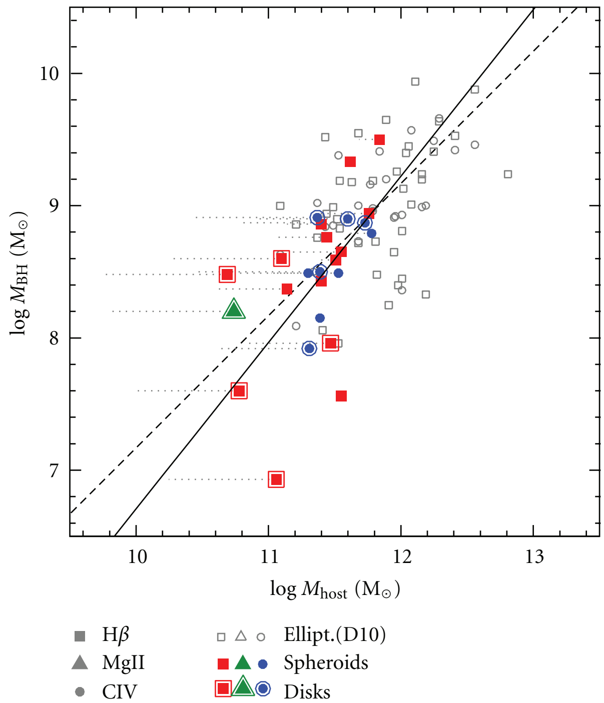

FIGURE 4: The M_{BH}-M_{host} relation in the objects in our sample (filled symbols), as compared with the $z < 0.5$ sample from [58] (empty symbols) and the local relation ($M_{BH}/M_{host} = 0.0015$; see [9]). Squares, triangles, and circles refer to M_{BH} estimates derived from Hβ, Mg_{II}, and C_{IV} respectively. Our new data substantially extend the sampled range of the M_{BH}-M_{host} relation. The relation holds down to quasar host masses of $\sim 10^{11}\,M_\odot$ (BH masses of $\sim 10^8\,M_\odot$). There is no evidence of a population of objects lying *below* the relation, as claimed by [62]. The overall scatter of the M_{BH}-M_{host} relation is 0.44 dex, and it extends over 2 dex both in terms of host galaxy and BH mass. Dotted, horizontal lines show how our objects would move if the correction for the bulge-to-total luminosity ratio is taken into account (see the text for details). The solid line is the best fit to our data.

TABLE 4: Average values of the M_{BH}/M_{host} ratio in various subsets of our sample. (1) Subsample. (2) Number of objects. (3) Average value of log Γ. (4) Root Mean Square of log Γ.

Subsample (1)	N (2)	⟨log Γ⟩ dex (3)	RMS dex (4)
Without B/T correction			
ALL	87	−2.842	0.444
$M_{BH} \geq 10^9\,M_\odot$	33	−2.627	0.351
$M_{BH} < 10^9\,M_\odot$	54	−2.974	0.445
$M_{host} \geq 4 \times 10^{11}\,M_\odot$	49	−2.889	0.401
$M_{host} < 4 \times 10^{11}\,M_\odot$	38	−2.782	0.492
With B/T correction			
ALL	87	−2.697	0.524
$M_{BH} \geq 10^9\,M_\odot$	33	−2.623	0.356
$M_{BH} < 10^9\,M_\odot$	54	−2.886	0.603
$M_{bulge} \geq 4 \times 10^{11}\,M_\odot$	46	−2.886	0.419
$M_{bulge} < 4 \times 10^{11}\,M_\odot$	41	−2.485	0.554

6. Conclusions

We measured black hole masses and host galaxy luminosities in a sample of 25 low-redshift ($z < 0.5$) quasars selected to have modest ($< 10^9\,M_\odot$) black hole masses.

For each object we inferred stellar masses. This allowed us to significantly expand the sampled range of M_{host} and M_{BH} for quasars. We found the following.

(i) The M_{BH}-M_{host} relation holds over all the 2 dex both in terms of M_{BH} and M_{host}. The relation has a scatter of 0.44 dex; that is, the sampled parameter space is ~5 times larger.

(ii) The slope of the M_{BH}-M_{host} relation in quasars is consistent with unity (in a log-log plane), consistently with what observed in quiescent galaxies.

(iii) The scatter of the relation increases by ~0.9 dex at the low-mass end.

(iv) After applying a simplistic correction for the disc contribution in objects with low Sersic indexes, the slope of the M_{BH}-M_{host} relation is smaller but still consistent with the linear case.

(v) No evidence of a population of quasars with relatively modest M_{BH} and very high M_{host} values is found.

Further studies at even lower M_{BH} masses ($\lesssim 10^7\,M_\odot$) and at higher redshift could provide further constraints on the early black hole growth and the nature of the seeds, and to pin down the evolution of the M_{BH}-host galaxy relations along the Cosmic Time. This requires extremely high-quality imaging of quasar host galaxies that would become possible with the next generation of ELT and laser assisted AO imagers.

Acknowledgments

R. Decarli acknowledges funding from Germany's national research center for aeronautics and space (DLR, project FKZ 50 OR 1104), based on observations made with the Nordic Optical Telescope, operated on the island of La Palma jointly by Denmark, Finland, Iceland, Norway, and Sweden, in the Spanish Observatorio del Roque de los Muchachos of the Instituto de Astrofisica de Canarias. This research has made use of the NASA/IPAC Extragalactic Database (NED) which is operated by the Jet Propulsion Laboratory, California Institute of Technology, under contract with the National Aeronautics and Space Administration. (Facilities: NOT (NOTCAM) SDSS HST).

References

[1] J. Kormendy and D. Richstone, "Inward bound—the search for supermassive black holes in galactic nuclei," *Annual Review of Astronomy and Astrophysics*, vol. 33, no. 1, pp. 581–624, 1995.

[2] R. Decarli, G. Gavazzi, I. Arosio et al., “The census of nuclear activity of late-type galaxies in the Virgo cluster,” *Monthly Notices of the Royal Astronomical Society*, vol. 381, no. 1, pp. 136–150, 2007.

[3] E. Gallo, T. Treu, J. Jacob, J. H. Woo, P. J. Marshall, and R. Antonucci, “Amuse-Virgo—I. Supermassive black holes in low-mass spheroids,” *Astrophysical Journal*, vol. 680, no. 1, pp. 154–168, 2008.

[4] K. Gebhardt, R. Bender, G. Bower et al., “A relationship between nuclear black hole mass and galaxy velocity dispersion,” *Astrophysical Journal*, vol. 539, no. 1, pp. L13–L16, 2000.

[5] L. Ferrarese and D. Merritt, “A fundamental relation between supermassive black holes and their host galaxies,” *Astrophysical Journal*, vol. 539, no. 1, pp. L9–L12, 2000.

[6] K. Gültekin, D. O. Richstone, K. Gebhardt et al., “The M-σ and M-L relations in galactic bulges, and determinations of their intrinsic scatter,” *Astrophysical Journal*, vol. 698, no. 1, pp. 198–221, 2009.

[7] A. W. Graham, C. A. Onken, E. Athanassoula, and F. Combes, “An expanded Mbh-σ diagram, and a new calibration of active galactic nuclei masses,” *Monthly Notices of the Royal Astronomical Society*, vol. 412, no. 4, pp. 2211–2228, 2011.

[8] J. Magorrian, S. Tremaine, D. Richstone et al., “The demography of massive dark objects in galaxy centers,” *Astronomical Journal*, vol. 115, no. 6, pp. 2285–2305, 1998.

[9] A. Marconi and L. K. Hunt, “The relation between black hole mass, bulge mass, and near-Infrared luminosity,” *Astrophysical Journal Letters*, vol. 589, no. 1, pp. L21–L24, 2003.

[10] N. Häring and H.-W. Rix, “On the black hole mass-bulge mass relation,” *Astrophysical Journal Letters*, vol. 604, no. 2, pp. L89–L92, 2004.

[11] J. Silk and M. J. Rees, “Quasars and galaxy formation,” *Astronomy and Astrophysics*, vol. 331, no. 2, pp. L1–L4, 1998.

[12] G. Kauffmann and M. Haehnelt, “A unified model for the evolution of galaxies and quasars,” *Monthly Notices of the Royal Astronomical Society*, vol. 311, no. 3, pp. 576–588, 2000.

[13] A. King, “The AGN-starburst connection, galactic superwinds, and M BH-σ,” *Astrophysical Journal*, vol. 635, no. 2, pp. L121–L123, 2005.

[14] J. S. B. Wyithe and A. Loeb, “Constraints on the process that regulates the growth of supermassive black holes based on the intrinsic scatter in the Mbh-σsph relation,” *Astrophysical Journal*, vol. 634, no. 2 I, pp. 910–920, 2005.

[15] B. Robertson, L. Hernquist, T. J. Cox et al., “The evolution of the MBH-σ relation,” *Astrophysical Journal*, vol. 641, no. 1, pp. 90–102, 2006.

[16] P. F. Hopkins, L. Hernquist, T. J. Cox, B. Robertson, and E. Krause, “A theoretical interpretation of the black hole fundamental plane,” *Astrophysical Journal*, vol. 669, no. 1, pp. 45–66, 2007.

[17] F. Shankar, “The demography of supermassive black holes: growing monsters at the heart of galaxies,” *New Astronomy Reviews*, vol. 53, no. 4–6, pp. 57–77, 2009.

[18] R. K. Malbon, C. M. Baugh, C. S. Frenk, and C. G. Lacey, “Black hole growth in hierarchical galaxy formation,” *Monthly Notices of the Royal Astronomical Society*, vol. 382, no. 4, pp. 1394–1414, 2007.

[19] T. Di Matteo, V. Springel, and L. Ilernquist, “Energy input from quasars regulates the growth and activity of black holes and their host galaxies,” *Nature*, vol. 433, no. 7026, pp. 604–607, 2005.

[20] G. Canalizo, N. Bennert, B. Jungwiert et al., “Spectacular shells in the host galaxy of the QSO MC2 1635 + 119,” *Astrophysical Journal*, vol. 669, no. 2, pp. 801–809, 2007.

[21] N. Bennert, G. Canalizo, B. Jungwiert et al., “Evidence for merger remnants in early-type host galaxies of low-Redshift QSOs,” *Astrophysical Journal*, vol. 677, no. 2, pp. 846–857, 2008.

[22] M. Cisternas, K. Jahnke, K. J. Inskip et al., “The bulk of the black hole growth since z∼1 occurs in a secular universe: no major merger-AGN connection,” *Astrophysical Journal Letters*, vol. 726, no. 2, article 57, 2011.

[23] B. M. Peterson and A. Wandel, “Evidence for supermassive black holes in active galactic nuclei from emission-line reverberation,” *Astrophysical Journal*, vol. 540, no. 1, pp. L13–L16, 2000.

[24] M. Vestergaard, “Determining central black hole masses in distant active galaxies,” *Astrophysical Journal*, vol. 571, no. 2, pp. 733–752, 2002.

[25] M. Vestergaard and B. M. Peterson, “Determining central black hole masses in distant active galaxies and quasars—II. Improved optical and UV scaling relationships,” *Astrophysical Journal*, vol. 641, no. 2, pp. 689–709, 2006.

[26] R. Decarli, R. Falomo, A. Treves, J. K. Kotilainen, M. Labita, and R. Scarpa, “The quasar MBH-Mhost relation through cosmic time—I. Data set and black hole masses,” *Monthly Notices of the Royal Astronomical Society*, vol. 402, no. 4, pp. 2441–2452, 2010.

[27] Y. Shen, G. T. Richards, M. A. Strauss et al., “A catalog of quasar properties from Sloan Digital Sky Survey Data Release 7,” *Astrophysical Journal*, vol. 194, no. 2, article 45, 2011.

[28] C. J. Willott, R. J. McLure, and M. J. Jarvis, “A 3 × 109 M⊙ black hole in the quasar SDSS J1148 + 5251 at z = 6.41,” *Astrophysical Journal*, vol. 587, no. 1, pp. L15–L18, 2003.

[29] J. D. Kurk, F. Walter, X. Fan et al., “Black hole masses and enrichment of z ∼ 6 SPSS quasars,” *Astrophysical Journal*, vol. 669, no. 1, pp. 32–44, 2007.

[30] C. J. Willott, L. Albert, D. Arzoumanian et al., “Eddington-limited accretion and the black hole mass function at redshift 6,” *Astronomical Journal*, vol. 140, no. 2, pp. 546–560, 2010.

[31] G. De Rosa, R. Decarli, F. Walter et al., “Evidence for non-evolving fe II/Mg II ratios in rapidly accreting z∼6 QSOs,” *Astrophysical Journal*, vol. 739, no. 2, article 56, 2011.

[32] A. Marconi, D. J. Axon, R. Maiolino et al., “On the observed distributions of black hole masses and eddington ratios from radiation pressure corrected virial indicators,” *The Astrophysical Journal Letters*, vol. 698, article L103, 2009.

[33] R. Decarli, M. Dotti, M. Fontana, and F. Haardt, “Are the black hole masses in narrow-line Seyfert 1 galaxies actually small?” *Monthly Notices of the Royal Astronomical Society*, vol. 386, no. 1, pp. L15–L19, 2008.

[34] R. Decarli, M. Dotti, and A. Treves, “Geometry and inclination of the broad-line region in blazars,” *Monthly Notices of the Royal Astronomical Society*, vol. 416, no. 1, 2011.

[35] H. Netzer, P. Lira, B. Trakhtenbrot, O. Shemmer, and I. Cury, “Black hole mass and growth rate at high redshift,” *Astrophysical Journal*, vol. 671, no. 2, pp. 1256–1263, 2007.

[36] R. Decarli, M. Labita, A. Treves, and R. Falomo, “On the geometry of broad emission region in quasars,” *Monthly Notices of the Royal Astronomical Society*, vol. 387, no. 3, pp. 1237–1247, 2008.

[37] M. Labita, R. Decarli, A. Treves, and R. Falomo, “Downsizing of supermassive black holes from the SDSS quasar survey—II. Extension to z ∼ 4,” *Monthly Notices of the Royal Astronomical Society*, vol. 399, no. 4, pp. 2099–2106, 2009.

[38] S. Fine, M. J. Jarvis, and T. Mauch, “Orientation effects in quasar spectra: the broad- and narrow-line regions,” *Monthly Notices of the Royal Astronomical Society*, vol. 412, no. 1, pp. 213–222, 2011.

[39] G. T. Richards, N. E. Kruczek, S. C. Gallagher et al., "Unification of luminous type 1 quasars through C_{iv} emission," *Astronomical Journal*, vol. 141, no. 5, article 167, 2011.

[40] J. K. Kotilainen, R. Falomo, R. Decarli, A. Treves, M. Uslenghi, and R. Scarpa, "The properties of quasar hosts at the peak of the quasar activity," *Astrophysical Journal*, vol. 703, no. 2, pp. 1663–1671, 2009.

[41] T. A. Targett, J. S. Dunlop, and R. J. McLure, "The host galaxies and black-hole:galaxy mass ratios of luminous quasars at z∼4," *Monthly Notices of the Royal Astronomical Society*. In press.

[42] R. Falomo, J. K. Kotilainen, R. Scarpa, and A. Treves, "VLT adaptive optics imaging of QSO host galaxies and their close environment at z ∼ 2.5: results from a pilot program," *Astronomy and Astrophysics*, vol. 434, no. 2, pp. 469–473, 2005.

[43] S. M. Croom, D. Schade, B. J. Boyle, T. Shanks, L. Miller, and R. J. Smith, "Gemini imaging of QSO host galaxies at z ∼ 2," *Astrophysical Journal*, vol. 606, no. 1 I, pp. 126–138, 2004.

[44] J. N. Bahcall, S. Kirhakos, D. H. Saxe, and D. P. Schneider, "Hubble Space Telescope images of a sample of 20 nearby luminous quasars," *Astrophysical Journal*, vol. 479, no. 2, pp. 642–658, 1997.

[45] M. J. Kukula, J. S. Dunlop, R. J. McLure et al., "A NICMOS imaging study of high-z quasar host galaxies," *Monthly Notices of the Royal Astronomical Society*, vol. 326, no. 4, pp. 1533–1546, 2001.

[46] S. E. Ridgway, T. M. Heckman, D. Calzetti, and M. Lehnert, "NICMOS imaging of the host galaxies of z ∼ 2-3 radio-quiet quasars," *Astrophysical Journal*, vol. 550, no. 1, pp. 122–141, 2001.

[47] T. S. Hamilton, S. Casertano, and D. A. Turnshek, "The luminosity function of QSO host galaxies," *Astrophysical Journal*, vol. 576, no. 1, pp. 61–74, 2002.

[48] J. S. Dunlop, R. J. McLure, M. J. Kukula, S. A. Baum, C. P. O'Dea, and D. H. Hughes, "Quasars, their host galaxies and their central black holes," *Monthly Notices of the Royal Astronomical Society*, vol. 340, no. 4, pp. 1095–1135, 2003.

[49] D. J. E. Floyd, M. J. Kukula, J. S. Dunlop et al., "The host galaxies of luminous quasars," *Monthly Notices of the Royal Astronomical Society*, vol. 355, no. 1, pp. 196–220, 2004.

[50] C. Y. Peng, C. D. Impey, L. C. Ho, E. J. Barton, and H. W. Rix, "Probing the coevolution of supermassive black holes and quasar host galaxies," *Astrophysical Journal*, vol. 640, no. 1, pp. 114–125, 2006.

[51] M. Kim, L. C. Ho, C. Y. Peng, A. J. Barth, and M. Im, "Decomposition of the host galaxies of active galactic nuclei using hubble space telescope images," *Astrophysical Journal*, vol. 179, no. 2, pp. 283–305, 2008.

[52] K. Jahnke, A. Bongiorno, M. Brusa et al., "Massive galaxies in cosmos: evolution of black hole versus bulge mass but not versus total stellar mass over the last 9 Gyr?" *Astrophysical Journal Letters*, vol. 706, no. 2, pp. L215–L220, 2009.

[53] V. N. Bennert, M. W. Auger, T. Treu, J.-H. Woo, and M. A. Malkan, "The relation between black hole mass and host spheroid stellar mass out to z∼2," *Astrophysical Journal*, vol. 742, no. 2, 2011.

[54] Y.-F. Jiang, J. E. Greene, and L. C. Ho, "Black hole mass and bulge luminosity for low-mass black holes," *Astrophysical Journal Letters*, vol. 737, no. 2, 2011.

[55] R. J. McLure, M. J. Jarvis, T. A. Targett, J. S. Dunlop, and P. N. Best, "On the evolution of the black hole: spheroid mass ratio," *Monthly Notices of the Royal Astronomical Society*, vol. 368, no. 3, pp. 1395–1403, 2006.

[56] C. Y. Peng, C. D. Impey, H. W. Rix et al., "Probing the coevolution of supermassive black holes and galaxies using gravitationally lensed quasar hosts," *Astrophysical Journal*, vol. 649, no. 2, pp. 616–634, 2006.

[57] A. Merloni, A. Bongiorno, M. Bolzonella et al., "On the cosmic evolution of the scaling relations between black holes and their host galaxies: broad-line active galactic nuclei in the zCosmos survey," *Astrophysical Journal*, vol. 708, no. 1, pp. 137–157, 2010.

[58] R. Decarli, R. Falomo, A. Treves, M. Labita, J. K. Kotilainen, and R. Scarpa, "The quasar MBH-Mhost relation through cosmic time—II. Evidence for evolution from z = 3 to the present age," *Monthly Notices of the Royal Astronomical Society*, vol. 402, no. 4, pp. 2453–2461, 2010.

[59] F. Walter, F. Bertoidl, C. Carilli et al., "Molecular gas in the host galaxy of a quasar at redshift z = 6.42," *Nature*, vol. 424, no. 6947, pp. 406–408, 2003.

[60] F. Walter, C. Carilli, F. Bertoldi et al., "Resolved molecular gas in a quasar host galaxy at redshift z = 6.42," *Astrophysical Journal*, vol. 615, no. 1, pp. L17–L20, 2004.

[61] M. Volonteri and P. Natarajan, "Journey to the MBH-σ relation: the fate of low-mass black holes in the universe," *Monthly Notices of the Royal Astronomical Society*, vol. 400, no. 4, pp. 1911–1918, 2009.

[62] D. Batcheldor, "The $M\bullet$-$\sigma*$ relation derived from sphere of influence arguments," *Astrophysical Journal*, vol. 711, no. 2, pp. L108–L111, 2010.

[63] J. E. Greene and L. C. Ho, "Active galactic nuclei with candidate intermediate-mass black holes," *Astrophysical Journal*, vol. 610, no. 2, pp. 722–736, 2004.

[64] J. E. Greene and L. C. Ho, "A new sample of low-mass black holes in active galaxies," *Astrophysical Journal Letters*, vol. 670, no. 1, pp. 92–104, 2007.

[65] X. Dong, T. Wang, W. Yuan et al., "Broad-line AGNs with Candidate intermediate-mass black holes in the sloan digital sky survey," in *Proceedings of the Central Engine of Active Galactic Nuclei*, vol. 373 of *ASP Conference Series*, p. 57, 2007.

[66] C. E. Thornton, A. J. Barth, L. C. Ho, R. E. Rutledge, and J. E. Greene, "The host galaxy and central engine of the dwarf active galactic nucleus POX 52," *Astrophysical Journal*, vol. 686, no. 2, pp. 892–910, 2008.

[67] T. Xiao, A. J. Barth, J. E. Greene et al., "The sloan digital sky survey: technical summary," *The Astronomical Journal*, vol. 120, p. 1579, 2000.

[68] D. G. York, J. Adelman, J. E. Anderson Jr. et al., "The Sloan Digital Sky Survey: Technical Summary," *Astronomical Journal*, vol. 120, p. 1579, 2000.

[69] M.-P. Veron-Cetty and P. Veron, "A catalogue of quasars and active nuclei: 13th edition," *Astronomy and Astrophysics*, vol. 518, article 10, 2010.

[70] I. N. Evans and A. P. Koratkar, "A complete atlas of recalibrated Hubble Space Telescope Faint Object Spectrograph spectra of active galactic nuclei and quasars—I. Pre-costar spectra," *Astrophysical Journal*, vol. 150, no. 1, pp. 73–164, 2004.

[71] F. Mannucci, F. Basile, B. M. Poggianti et al., "Near-infrared template spectra of normal galaxies: k-corrections, galaxy models and stellar populations," *Monthly Notices of the Royal Astronomical Society*, vol. 326, no. 2, pp. 745–758, 2001.

[72] M. Vestergaard and B. J. Wilkes, "An empirical ultraviolet template for iron emission in quasars as derived from I Zwicky 1," *Astrophysical Journal*, vol. 134, no. 1, pp. 1–33, 2001.

[73] M. Uslenghi and R. Falomo, "AIDA: astronomical image decomposition and analysis," *Modelling and Simulation In Science*, pp. 313–318, 2008.

[74] J. K. Kotilainen, R. Falomo, M. Labita, A. Treves, and M. Uslenghi, “The nuclear to host galaxy relation of high-redshift quasars,” *Astrophysical Journal*, vol. 660, no. 2 I, pp. 1039–1050, 2007.

[75] L. Simard, J. Trevor Mendel, D. R. Patton, S. L. Ellison, and A. W. McConnachie, “A catalog of bulge+disk decompositions and updated photometry for 1.12 million galaxies in the Sloan digital sky survey,” *Astrophysical Journal*, vol. 196, no. 1, article 11, 2011.